Lavendamycin Antitumor Agents: Structure-Based Design, Synthesis, and NAD(P)H:Quinone Oxidoreductase 1 (NQO1) Model Validation with Molecular Docking and Biological Studies

Mary Hassani,[†] Wen Cai,[‡] Katherine H. Koelsch,[†] David C. Holley,[§] Anthony S. Rose,[‡] Fatemeh Olang,[‡] Jayana P. Lineswala,[‡] William G. Holloway,[‡] John M. Gerdes,[§] Mohammad Behforouz,*[,‡] and Howard D. Beall*[,†]

Center for Environmental Health Sciences, Department of Biomedical and Pharmaceutical Sciences, The University of Montana, Missoula, Montana 59812, Molecular Computational Core Facility, Center for Structural and Functional Neuroscience, Department of Biomedical and Pharmaceutical Sciences, The University of Montana, Missoula, Montana 59812, Department of Chemistry, Ball State University, Muncie, Indiana 47306

Received August 28, 2007

A 1H69 crystal structure-based in silico model of the NAD(P)H:quinone oxidoreductase 1 (NQO1) active site has been developed to facilitate NQO1-directed lavendamycin antitumor agent development. Lavendamycin analogues were designed as NQO1 substrates utilizing structure-based design criteria. Computational docking studies were performed using the model to predict NQO1 substrate specificity. Designed *N*-acyllavendamycin esters and amides were synthesized by Pictet−Spengler condensation. Metabolism and cytotoxicity studies were performed on the analogues with recombinant human NQO1 and human colon adenocarcinoma cells (NQO1-deficient BE and NQO1-rich BE-NQ). Docking and biological data were found to be correlated where analogues **12**, **13**, **14**, **15**, and **16** were categorized as good, poor, poor, poor, and good NQO1 substrates, respectively. Our results demonstrated that the ligand design criteria were valid, resulting in the discovery of two good NQO1 substrates. The observed consistency between the docking and biological data suggests that the model possesses practical predictive power.

Introduction

NQO1[a] is a widely distributed homodimeric flavoenzyme composed of two closely associated monomers of 273 residues, each containing one molecule of FAD cofactor that is required for NQO1 catalytic activity.[1–5] NQO1 catalyzes an NAD(P)H-dependent, two-electron reduction of quinones.[6,7] A number of quinone-based chemotherapeutic agents including quinolinequinones, such as our previously studied lavendamycin analogues[8] and streptonigrin,[9–11] mitomycin C,[12,13] β-lapachone (a 1,2-naphthoquinone analogue),[14,15] and various indolequinones[16–18] and aziridinylbenzoquinones,[19–25] can be bioactivated by NQO1. NQO1 overexpression in many human solid tumors has been established,[26–30] and NQO1 is considered a key target for the design of quinone-based chemotherapeutic agents that can be bioactivated by the enzyme to achieve selective toxicity toward NQO1-rich tumors.

Lavendamycin (**1**) (Chart 1), a naturally occurring 7-aminoquinoline-5,8-dione antitumor antibiotic, was first isolated from the fermentation broth of *Streptomyces lavendulae* by Balitz et al.,[31] and its structure was determined by Doyle et al.[32] The latter study determined that **1** is a pentacyclic structure with two moieties including quinoline-5,8-dione and indolopyridine (β-carboline) (Chart 1).[32] Compound **1** has been the focus of several synthetic studies to elucidate the structural features that are required for its cytotoxic activity and to develop improved analogues with potent antitumor properties and lower animal toxicity. Initial SAR studies have demonstrated that the essential

Chart 1

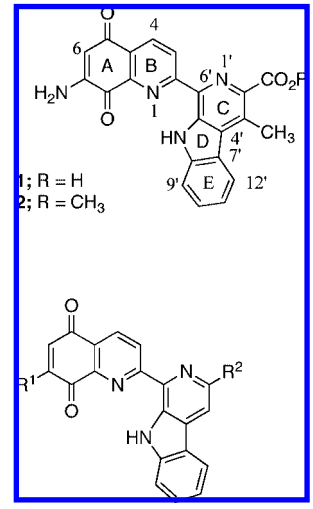

moiety for the cytotoxic activity of **1** is the 7-aminoquinoline-5,8-dione moiety.[33] It has also been reported that lavendamycin analogues possess low animal toxicity.[34,35]

Bioreductive enzyme-directed antitumor agent development depends on the identification of chemotherapeutic agents with high substrate specificity for target reductases.[36] Structure-based ligand design is an efficient approach in modern drug development for targets with resolved three-dimensional structures.[37–39] In structure-based design, the information obtained from the interactions and composite structure of the target protein–ligand is utilized to design improved ligands with high binding affinity for target proteins implicated in diseases.[37–40] Deeper insight of ligand−protein interactions within the active site of the target greatly contributes to more refined SAR studies, which in turn are the crucial components in the context of structure-based ligand design.[41] Computer-aided docking techniques serve as

* Corresponding authors for chemistry (M.B.) and biology (H.D.B.). M. Behforouz: Phone, 765-285-8070; Fax, 765-285-6505; E-mail, mbehforo@bsu.edu. H. D. Beall: Phone, 406-243-5112; Fax, 406-243-5228; E-mail, howard.beall@umontana.edu.

[†] Center for Environmental Health Sciences, The University of Montana.

[§] Molecular Computational Core Facility, The University of Montana.

[‡] Department of Chemistry, Ball State University.

[a] Abbreviations: FAD, flavin adenine dinucleotide; NQO1, NAD(P)H: quinone oxidoreductase 1; RMSD, root-mean-square deviation; SAR, structure–activity relationship.

10.1021/jm701066a CCC: $40.75
Published on Web 05/06/2008

Table 1. Structures of Lavendamycin Analogues, Yields, and Reaction Conditions

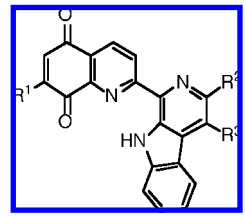

no.	R^1	R^2	R^3	% yield	solvent	h (°C)[a]
11	CH_3CONH	$CO_2(CH_2)_2OH$	H	87–94	DMF/anisole	2 (reflux)[35]
12	CH_3CONH	$CONH(CH_2)_3CH_3$	H	43	anisole	20 (reflux)
13	CH_3CONH	$CONHCH(CH_3)C_2H_5$	H	35	anisole	15 (reflux)
14	*n*-C_3H_7CONH	$CO_2(CH_2)_2CH(CH_3)_2$	H	70	xylene	17 (reflux)[34]
15	2-furylCONH	CO_2CH_3	H	53.5	xylene	17 (reflux)
16	NH_2	$CO_2(CH_2)_2OH$	H	30	hydrolysis of **11**	
28	NH_2	$CO_2C_8H_{17}$-*n*	H		see ref 35	
29	NH_2	CH_2OH	H		see ref 8	
30	CH_3CONH	$CO_2C_5H_{11}$-*i*	H		see ref 8	
31	NH_2	$CONH_2$	H		see ref 35	

[a] For the synthesis of **11–15**, the reaction mixtures were slowly heated to reflux over a period of approximately 3 h. Compound **16** was obtained by the acid hydrolysis of **11** and **28–31** were synthesized according to our previously reported methods.

time- and cost-efficient tools for structure-based design making for more efficient syntheses and biological testing of new analogues.[38,42] These techniques greatly contribute to this field because they facilitate a greater understanding of the binding events and the molecular basis of ligand−protein interactions as well as prediction of binding orientations and affinities of candidate compounds.[37–39,43] The information is then utilized to design more efficacious new analogues.[38]

Crystal structure complexes with bound ligands and cofactors can be used as composite reference structures for docking studies and the creation of active site models.[37,38,40] The crystal structures of the apo human NQO1[1,4] and human NQO1 in complex with several agents have been reported.[4,44–46] The active site of the enzyme is a hydrophobic and plastic pocket capable of forming van der Waals and hydrogen bond interactions with quinone compounds.[4,8,45] The substrate binding pocket sequentially binds NAD(P)H and the quinone substrate during an obligatory two-electron reduction process (ping-pong mechanism).[4,5,45] During this process, a hydride ion from NAD(P)H is transferred to the N5 of the FAD followed by the release of $NAD(P)^+$.[5,47,48] The hydride donation from the FAD N5 to the hydride-acceptor quinone can then be accomplished followed by hydroquinone release.[5,45,47,48] NQO1 crystal structure-based molecular modeling studies have been recommended for structure-based design efforts for the optimization of quinone antitumor agents.[4,45,49]

Complete synthesis of the methyl ester of lavendamycin (**2**) (Chart 1) was first reported by Kende et al. in 1984,[50] and the second synthesis of this compound was described by Boger et al. in 1985.[51] However, our 1993[52] and 1996[53] reported syntheses of **2** are much shorter and more efficient compared to the methods reported by the first two groups.[50,51] Because of the practicality of our synthetic methods, specifically that reported in 1996,[53] we have been able to synthesize a large number of substituted lavendamycins and study their various biological activities.[8,34,35,54] In this report, we describe the synthesis of rationally designed analogues **12**, **13**, **15**, and **16** (Table 1).

The present study was conducted to design more optimal lavendamycin substrates for NQO1 with increased selective cytotoxicity toward NQO1-rich cells using computational active site docking studies and correlated SAR data. The objective was to determine whether our design criteria were valid and whether docking data acquired using our recently developed in silico model of the NQO1 active site were consistent with the biological data. We also sought to investigate the predictive power of the model to correctly distinguish between good and poor NQO1 substrates. This is the first study to perform structure-based lavendamycin analogue design using molecular docking and SAR data that serve to validate the developed model with computational and biological studies.

Results and Discussion

Structure-Based Design. Lavendamycin analogues **12**, **13**, **15**, and **16** (Table 1) were designed utilizing the criteria obtained from our previous SAR and modeling study[8] and other recent NQO1-related literature. The structure-based design criteria for substituents at key ligand positions (Chart 1) are discussed in the following sections.

Quinolinedione-7 Position (R^1). (1) Substituents should be small to medium in size, preferably NH_2 or $NHCOCH_3$ groups,[8] that do not produce steric interactions with the key residues of the active site including the internal wall (Trp-105/Phe-106) (applied to **12**, **13**, and **16**).[40,55,56] The substituents should also be capable of hydrogen bond formation with the FAD cofactor and/or the key amino acid residues of the active site including Tyr-126, -128, and His-161.[8] Faig et al. determined that positions of **24** (RH1; Chart 2), 2,5-diaziridinyl-3-(hydroxymethyl)-6-methyl-1,4-benzoquinone,[25] that point to the inner part of the NQO1 active site could accommodate only small substituents.[45] (2) Substituents that can intercalate between and/or form van der Waals interactions with the Trp-105/Phe-106 minipocket (applied to **15**).[40,55] A previous study demonstrated that an aziridinyl group at the C5 position of **25** (EO9; Chart 2), 3-hydroxymethyl-5-aziridinyl-1-methyl-2-(1H-indole-4,7-dione)-propenol,[57] can form favorable van der Waals interactions with Trp-105.[55] Additionally, van der Waals interactions between the C5 aziridine ring of **26** (CB1954; Chart 2), 5-aziridinyl-2,4-dinitrobenzamide,[1] and Trp-105 are important to the binding of this prodrug.[1] Unsubstituted pyrrolo and pyrido rings in dipyrroloimidazobenzimidazole and dipyridoimidazobenzimidazole compounds are able to sandwich between Trp-105/Phe-106 residues and form van der Waals interactions to increase NQO1 substrate specificity.[40] (3) No large substituents are allowed due to increased steric hindrance with the internal

Chart 2

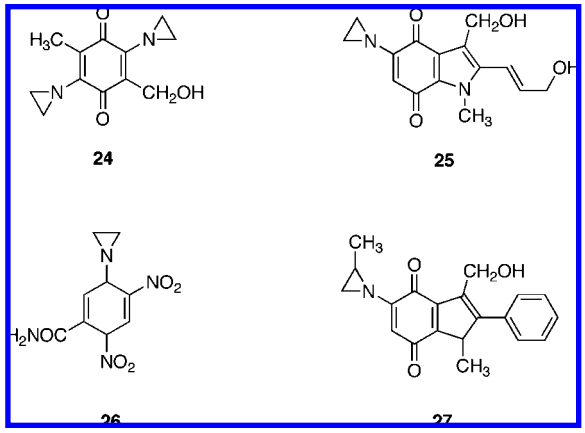

wall that can result in unfavorable positioning of the quinoline-5,8-dione moiety of lavendamycin analogues for hydride ion reception from FAD and quinone reduction (applied to **12**, **13**, **15**, and **16**).[8,40] A study by Suleman et al. demonstrated that dipyrroloimidazobenzimidazole compounds with both pyrrolo rings bearing bulky substituents were excluded from the active site due to steric interactions.[40]

Quinolinedione-6 Position. Absence of substituents in this position is highly preferred. The simultaneous placement of substituents at both R^1 and the quinolinedione-6 position increases steric interactions of the lavendamycin ligands with the internal wall of the active site.[8] It has been reported that 1,4-naphthoquinones with small substituents such as an aziridine ring or CH_3 at C2 and no substituents at C3 (C2 and C3 positions point to the inside of the active side) are good substrates for NQO1.[58] Increased bulkiness of substituents at the C5 position of indolequinones dramatically reduced rates of reduction by NQO1.[45,55] Previous SAR studies have demonstrated that 7-aminoquinoline-5,8-dione is an essential moiety in determining the cytotoxic and antitumor activity of quinolinedione antibiotics.[33,59] Therefore, substituent placement at the R^1 position over quinolinedione-6-position is highly desirable (applied to **12**, **13**, **15**, and **16**).

Indolopyridine-2′ Position (R^2). (1) Substituents should be capable of hydrogen bond formation with the FAD cofactor and/or the key residues of the active site including Gly-149 and Gly-150 (applied to **15** and **16**).[8] The 3-hydroxymethyl group of **27** (ARH019; Chart 2), 3-(hydroxymethyl)-5-(2-methylaziridin-1-yl)-1-methyl-2-phenylindole-4,7-dione,[18] that points toward the outside of the active site forms a hydrogen bond with the Tyr-128 OH.[45] (2) Substituents (including aliphatic chains) should be capable of formation of van der Waals interactions with residues of the NQO1 active site (applied to **12** and **13**). Compound **28**, demethyllavendamycin *n*-octyl ester,[35] possesses a large *n*-octyl ester substituent at the R^2 position and is a good NQO1 substrate with high selective toxicity toward NQO1-rich cancer cells.[8]

Utilizing the above criteria, we designed compounds **12**, **13**, **15**, and **16** with small or medium size substituents at R^1, no substituent at quinolinedione-6-position, and small to large substituents at R^2. The substituents at R^1 and R^2 were expected to form hydrogen bond and/or van der Waals interactions with FAD and/or the amino acid residues of the NQO1 active site such as Trp-105, Phe-106, Tyr-126, -128, −Gly-149, -150, and His-161. Docking studies with compounds **12**, **13**, **15**, and **16** using an X-ray derived, in silico model were performed to predict the substrate specificity of the compounds for NQO1, to examine the predictive power of the model, to relate the model and docking studies with the metabolism and cytotoxicity results, and to gain deeper insight into the binding events and the molecular basis of lavendamycin analogue−NQO1 interactions.

Synthetic Chemistry. Table 1 displays the structures of lavendamycin analogues **11**−**16** and **28**−**31**. Analogues **12**, **13**, **15**, and **16** were designed and synthesized. These lavendamycin analogues as well as previously synthesized compound **14** were the subject of our metabolism, cytotoxicity, and modeling studies in this report. As shown in Scheme 1, Pictet−Spengler condensation of 7-*N*-acylamino-2-formylquinoline-5,8-diones **3–5** with trytophan esters **6**, **9**, and **10** and amides **7** and **8** yielded the corresponding lavendamycin derivatives **11–15**. The synthesis of compounds **11**, **14**, and **28**−**31** has already been reported by us.[8,34,35]

Demethllavendamycin β-hydroxyethyl ester (**16**) was prepared by the acid hydrolysis of acetyl derivative **11** in 30% yield.

Aldehydes **3** and **4** necessary for the synthesis of lavendamycins **11–14** were prepared through our reported procedures.[35,53] Aldehyde **5** required for the synthesis of lavendamycin **15** was obtained via reactions shown in Scheme 2.

Tryptophan esters **6**, **9**, and **10** were prepared according to our previously reported method.[8,35] Tryptophan amides **7** and **8** were prepared according to Scheme 3, via similar methods to those previously reported by us.[8] Benzyloxycarbonyl succinimide ester **21** was obtained[8] and then condensed with *n*-butylamine or *s*-butylamine to produce **22** and **23** respectively in yields of 68 and 90%. Deprotection of **22** and **23** with dry ammonium formate in the presence of 10% Pd/C yielded tryptophan amides **7** and **8** in 77% and 75% yields, respectively.

Docking Studies. Our laboratory recently developed an 1H69 crystal structure-based in silico model of the NQO1 active site.[8] To further determine the predictive power of the model and correlation of the docking data with biological measures, we performed computational and comparative docking studies on the structure-based designed lavendamycin analogues **12**, **13**, **15**, and **16** and the previously synthesized compound **14**. The molecular modeling studies were performed using SYBYL 7.0 software suite[60] (Tripos, Inc., St. Louis, MO). Flexible docking was performed using the FlexX software module within the SYBYL environment, where FlexX is capable of determining 30 possible conformations (poses) for each docked ligand.[61,62] The docked conformations of ligands **12**−**16** were evaluated and ranked using the CSCORE module, with ranking scores between 0 and 5, where 5 was the best fit to the model. Table 2 displays the number of conformations of the ligands in each score group of CSCORE function.

Ligands **12** and **16** possessed higher number of poses with optimal CSCORE values compared to **13**, **14**, and **15** (Table 2). Visual screening of the binding orientations of the poses and geometric postdocking analyses were performed. The analyses included distance measurements and pose geometries that determined: (1) hydrogen-bonding and van der Waals interactions of ligand poses with FAD and the key residues of the NQO1 active site including Trp-105, Phe-106, Tyr-126, -128, Gly-149, -150, His-161, and Phe-232, and (2) hydride ion transfer from the N5 of the FAD isoalloxazine ring to the ligands at carbonyl oxygens (O5 or O8), ring carbon, or substituent atoms. Residue numbers in this paper are those used in the Protein Data Bank coordinates, PDB ID code: 1H69.[45] Only poses of the ligands with CSCORE ≥ 4 were considered for further detailed postdocking analyses.

Ligands **12** and **13** were designed to possess highly similar chemical structures with only a minor difference in the sub-

Scheme 1

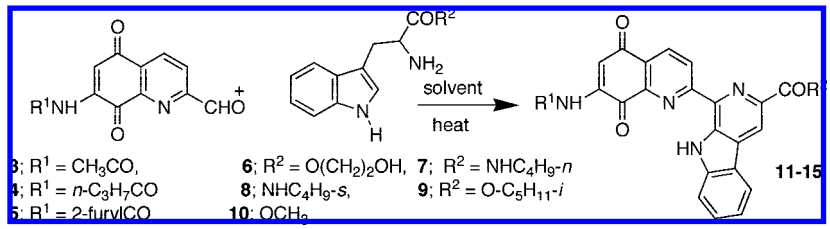

Scheme 2[a]

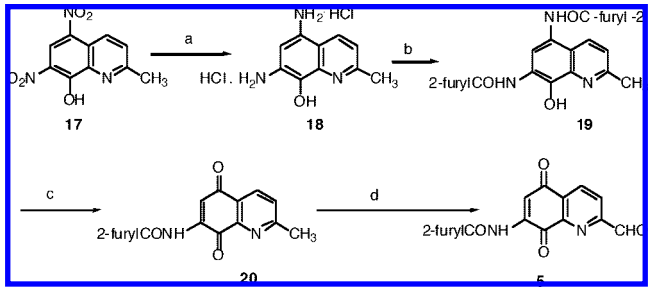

[a] Reagents and conditions: (a) Pd−C 5%, H_2 (41 psi), HCl−H_2O, 24 h, rt, 82%; (b) 2-furylCOCl, NaOAc, Na_2SO_3, 2 h, 0 °C, 75%; (c) $K_2Cr_2O_7$, HOAc, THF, H_2O 20 h, rt, 64%; (d) SeO_2, dioxane, 26 h, reflux, 93%.

Scheme 3[a]

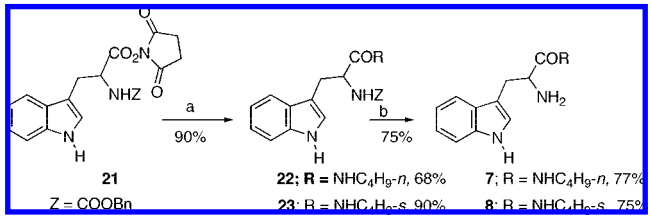

[a] Reagents and conditions: (a) *s*-butylamine, Et_3N, EtOH, $CHCl_3$, 2 h, rt; (b) dry MeOH, dried ammonium formate, 10% Pd/C, Ar, 30 min, rt.

Table 2. Number of Poses of Ligands **12**, **13**, **14**, **15**, and **16** in Each Score Group of CSCORE Function

	number of poses				
CSCORE	**12**	**13**	**14**	**15**	**16**
0	7	6	5	9	5
1	4	9	10	9	3
2	5	1	6	7	2
3	5	11	4	3	5
4	4	3	5	1	10
5	5	0	0	1	5

stituents at R^2 (R^2 substituents of **12** and **13** are structural isomers) in order to examine the role that R^2 substituents play in the affinity of lavendamycin substrates for NQO1. Ligand **12** possessed nine poses of CSCORE ≥ 4 compared to ligand **13**, with only three poses of CSCORE ≥ 4 (Table 2). Poses 1, 2, 4, 5, and 6 (CSCORE = 5) of **12** fell into one cluster in which the RMSD of the poses equaled zero for atoms of the quinolinedione and indolopyridine moieties, and the difference was in the binding orientation of the $CONH(CH_2)_3CH_3$ group in the NQO1 active site (Figure 1a). All of the poses of **12** entered the active site by the 5,8-dione moiety, where the carbonyl oxygen O8 compared to O5 was positioned closer to Tyr-126, -128, and FAD (Figure 1a and Table 3).[45,55] The binding orientations of the poses of **12** in the cluster are considered as preferred binding orientations of **12** because these are the binding orientations with maximum CSCORE = 5 (Figure 1a).

One crucial determining factor of NQO1 substrate binding strength in the NQO1 active site is the ability to form hydrogen-bonding and/or van der Waals interactions with FAD and/or amino acid residues of the active site.[1,40,45,47] Good substrates for NQO1 such as **24**, **25**, and **26** are capable of hydrogen-bonding interactions with the key amino acid residues of the NQO1 active site.[1,45] Duroquinone, a tetramethyl analogue of benzoquinone, binds to the NQO1 active site through interactions with FAD and several hydrophilic and hydrophobic residues.[4] For ligand **12**, poses 1, 2, 4, 5, and 6 formed the highest number of hydrogen bonds and van der Waals interactions in the active site of the enzyme. For pose 1 of **12**, the Tyr-128 OH formed hydrogen bonds with the carbonyl oxygen O8, the NH of the indole ring of the indolopyridine moiety, and the carbonyl oxygen of the quinolinedione-7 position substituent (Figure 1b). The carbonyl oxygen O5 formed a hydrogen bond with the NH of His-161 (Figure 1b). The NH of the quinolinedione-7 position substituent also formed hydrogen bonds with the N1, N5, and N10 of FAD (Figure 1b). The $CONH(CH_2)_3CH_3$ group of the indolopyridine moiety further stabilized the binding by forming van der Waals interactions with Phe-232 (Figure 1b). Poses 2, 4, 5, and 6 displayed the same interactions as pose 1 (only pose 1 is shown) (Figure 1b and Table 3). The docked model determined a high number of poses of **12** with optimum CSCORE (≥4) that are capable of hydrogen bond and van der Waals formation in the NQO1 active site, suggesting that this compound is a good substrate for NQO1.

However, of the thirty poses of **13**, only poses 1, 2, and 4 merited further considerations (CSCORE = 4), and the remainder of the poses possessed CSCORE ≤ 3 (Table 2). None of the poses of **13** had a CSCORE = 5 (Table 2). Poses 1, 2, and 4 of **13** entered the active site by the 5,8-dione moiety similar to the poses of **12** (Figure 2a and Table 4). Although these poses formed hydrogen bonds with FAD and the residues of the NQO1 active site, the number of total hydrogen bonds was lower than that for the poses of **12** (hydrogen bonds not shown). Furthermore, poses 1, 2, and 4 of **13** were found not to form van der Waals interactions with Phe-232, compared to the poses of **12**, providing a rationale for the lower binding affinity of **13** compared to **12** in the NQO1 active site (Figure 2a,b). The in silico docking studies ranked **13** as a poor substrate for NQO1. Overall, a higher number of more favorable poses of ligand **12** were found compared to **13** that formed key hydrogen bonding interactions (van der Waals interactions only in poses of **12**) and had favorable binding orientations for hydride ion reception and quinone reduction. The in silico model was found to be capable of distinguishing the differences between the respective good and poor NQO1 substrate qualities of **12** and **13**.

Compound **15** was designed to investigate whether an aromatic amide group at R^1 is capable of intercalating between Trp-105 and Phe-106 residues and forming van der Waals interactions to increase NQO1 substrate specificity. Docking studies of **15** were performed to observe how the model would

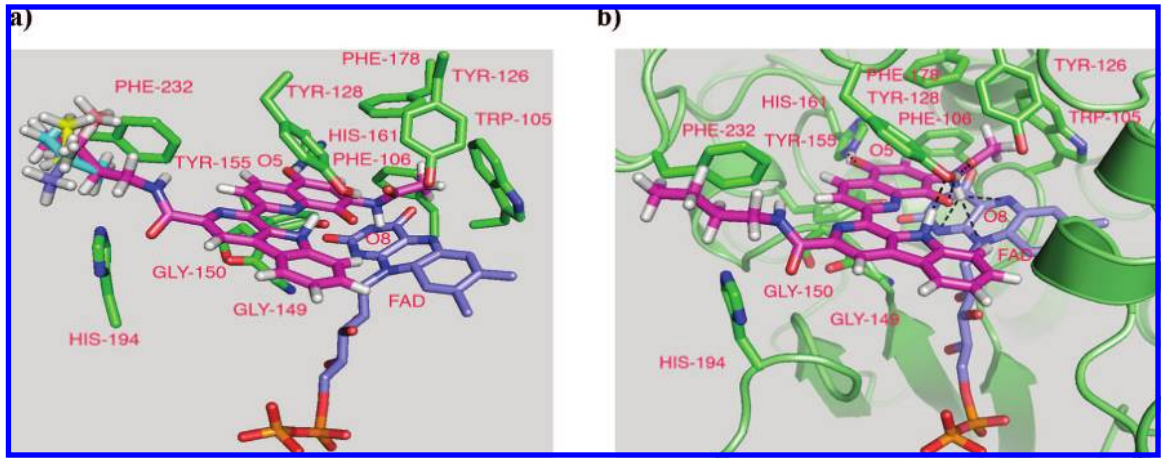

Figure 1. Molecular models of the poses of ligand **12** docked into the NQO1 active site. (a) View of the superposition of the docked poses 1, 2, 4, 5, and 6 of **12** (magenta, cyan, yellow, salmon, and blue, respectively) (CSCORE = 5) in the NQO1 active site. (b) Molecular model of the pose 1 of **12** (magenta) (CSCORE = 5) docked into the NQO1 active site. In (b) the Tyr-128 OH formed hydrogen bonds with the carbonyl oxygen O8, the NH of the indole ring of the indolopyridine moiety, and the carbonyl oxygen of the quinolinedione-7 position substituent. The carbonyl oxygen O5 formed a hydrogen bond with the NH of His 161. The NH of the quinolinedione-7 position substituent also formed hydrogen bonds with the N1, N5, and N10 of FAD. The $CONH(CH_2)_3CH_3$ group of the indolopyridine moiety further stabilized the binding by forming van der Waals interactions with Phe-232. In (a) and (b) residues of the active site (green), FAD (blue), and **12** are represented as stick models. In (b) the rest of the structure is represented as a secondary structure cartoon. The atoms are colored: red, oxygen atoms; blue, nitrogen atoms; orange, phosphorus atoms; and white, hydrogen atoms. Hydrogen bonds are represented as black dashed lines.

Table 3. Geometric Post-Docking Analysis and Measurements of Five Poses (CSCORE = 5) and Four Poses (CSCORE = 4) of Ligand **12** in the NQO1 Active Site

P[a]	C[b]	O5−Tyr-126 (Å)	O5−Tyr-128 (Å)	O8−Tyr-126 (Å)	O8−Tyr-128 (Å)	N5−O5 (Å)	N5−O8 (Å)	N5−C6 (Å)	N5−C7 (Å)
1	5	9.174	6.143	4.862	2.077	7.786	5.006	5.515	4.622
2	5	9.174	6.143	4.862	2.077	7.786	5.006	5.515	4.622
4	5	9.174	6.143	4.862	2.077	7.786	5.006	5.515	4.622
5	5	9.174	6.143	4.862	2.077	7.786	5.006	5.515	4.622
6	5	9.174	6.143	4.862	2.077	7.786	5.006	5.515	4.622
3	4	9.417	6.196	4.804	1.802	7.953	5.281	5.714	4.863
7	4	9.260	6.085	4.774	1.899	7.772	5.187	5.532	4.697
14	4	9.180	6.242	4.878	2.123	7.618	4.960	5.375	4.515
25	4	9.167	6.198	4.882	2.081	7.692	5.016	5.427	4.560

[a] P = Pose. [b] C = CSCORE.

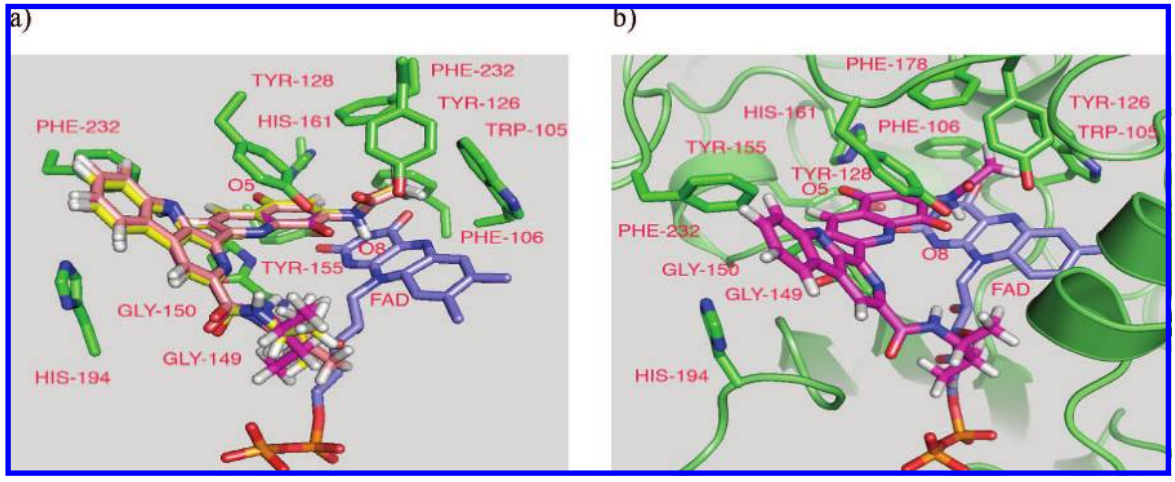

Figure 2. Molecular models of the poses of ligand **13** docked into the NQO1 active site. (a) View of the superposition of the docked poses 1, 2, and 4 of **13** (magenta, yellow, and salmon, respectively) (CSCORE = 4) in the NQO1 active site. (b) Molecular model of the pose 1 of **13** (magenta) (CSCORE = 4) docked into the NQO1 active site. In (a) and (b) residues of the active site (green), FAD (blue), and **13** are represented as stick models. In (b) the rest of the structure is represented as a secondary structure cartoon. The atoms are colored: red, oxygen atoms; blue, nitrogen atoms; orange, phosphorus atoms; and white, hydrogen atoms.

rank this compound as an NQO1 substrate. Only poses 7 and 30 of ligand **15** possessed CSCORE ≥ 4 (Table 2). These poses entered the active site by the 5,8-dione moiety similar to the poses of **12** (Supporting Information Figure 1a and Table 1). The other 28 poses with CSCORE ≤ 3 were found to be excluded from the NQO1 active site including pose 2 (CSCORE = 3) (only pose 2 is shown; Supporting Information Figure 1b). The NHCO-2-furyl group of poses 7 and 30 did not intercalate between the Trp-105 and Phe-106 residues, suggesting the lack of Van der Waals interactions with the Trp-105/Phe-106

Table 4. Geometric Post-Docking Analysis and Measurements of Three Poses of Ligand **13** (CSCORE = 4) in the NQO1 Active Site

P[a]	C[b]	O5−Tyr-126 (Å)	O5−Tyr-128 (Å)	O8−Tyr-126 (Å)	O8−Ty-r128 (Å)	N5−O5 (Å)	N5−O8 (Å)	N5−C6 (Å)	N5−C7 (Å)
1	4	9.402	6.193	4.802	1.828	7.933	5.246	5.689	4.831
2	4	9.402	6.193	4.802	1.828	7.933	5.246	5.689	4.831
4	4	9.268	6.084	4.692	1.770	7.739	5.240	5.504	4.691

[a] P = Pose. [b] C = CSCORE.

minipocket and presence of possible steric interactions with the residues Trp-105 and Phe-106 (Supporting Information Figure 1a). Previous studies have indicated that the Trp-105/Phe-106 minipocket can play a crucial role in impacting the substrate specificity of NQO1 ligands.[40,55,63] Our model ranked ligand **15** as a poor substrate for NQO1.

Compound **16** was designed after the good NQO1 substrate, compound **29**,[8] decarboxy-2′-(hydroxymethyl)-demethyllavendamycin,[8] to create another good substrate. Fifteen poses of ligand **16** were found to possess CSCORE values ≥4 (Table 2). Poses 1, 2, 4, and 7 (CSCORE = 5) of **16** entered the active site by the 5,8-dione moiety similar to the poses of **12** (Supporting Information Figure 2a and Table 2). Among five poses of **16** with CSCORE = 5, pose 8 entered the active site with an orientation opposite to poses 1, 2, 4, and 7 (Supporting Information Figure 2b and Table 2). Different binding orientations of quinone substrates that can facilitate hydride ion reception from the FAD N5 to the substrates can be tolerated in the active site.[45,47] Among the poses of ligand **16**, poses 1, 2, 4, and 7 formed the highest number of hydrogen bonds in the active site of the enzyme (for a detailed description of hydrogen bonds that were formed by ligand **16**, see Supporting Information Figure 2c legend). Pose 8, among poses of **16** with CSCORE = 5, formed the lowest number of hydrogen bonds, suggesting that the binding orientations of poses 1, 2, 4, and 7 are the preferred binding orientations for ligand **16** relative to pose 8 (Supporting Information Figure 2a,b). Taken together, the in silico model recognized **16** as a good substrate for NQO1.

Compound **14** was selected from previously synthesized lavendamycin analogues, and according to our previous SAR studies,[8] this compound was thought to be a poor substrate for NQO1 due to the presence of the large $NHCOC_3H_7$-*n* group at the R^1 position that could create steric interactions inside the NQO1 active site. Therefore, compound **14** was selected for docking studies to observe how the model would rank it as an NQO1 substrate. None of the conformations of **14** had a CSCORE = 5 (Table 2), and all of the poses of **14**, including poses 2, 5, 6, 21, and 25 (CSCORE = 4), fell into one cluster that yielded an RMSD equal to 0 Å for atoms of the quinolinedione and indolopyridine moieties (Supporting Information Figure 3a). However, the binding orientations of the $NHCOC_3H_7$-*n* and $CO_2C_2H_4CH(CH_3)_2$ groups of **14** were found to be less optimal (Supporting Information Figure 3a), and all 30 poses of **14** were excluded from the NQO1 active site (only pose 2 is shown; Supporting Information Figure 3b). The site exclusion is most likely related to the steric hindrance produced by the large $NHCOC_3H_7$-*n* substituent against the Trp-105/Phe-106 wall that could be further enhanced by the contributing steric effect produced by the large $CO_2C_2H_4CH(CH_3)_2$ group at R^2. Ligand **14** was ranked as a poor substrate for NQO1 by the in silico model.

The molecular docking studies demonstrated that ligands **12** and **16** possessed an increased number of possible poses with optimal CSCORE values and favorable binding orientations to promote hydrogen bonding and van der Waals interactions, hydride ion reception, and quinone reduction compared to ligands **13**, **14**, and **15**.

Table 5. Metabolism of Lavendamycin Analogues by Recombinant Human NQO1 Monitored by Spectrophotometric Cytochrome *c* Assay

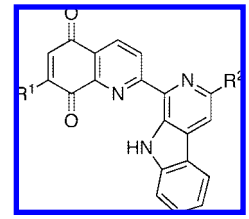

no.	R^1	R^2	metabolism by NQO1 (μmol/min/mg) (cytochrome *c* reduction)
12	CH_3CONH	$CONH(CH_2)_3CH_3$	143 ± 11
13	CH_3CONH	$CONHCH(CH_3)C_2H_5$	4.9 ± 2.9
14	*n*-C_3H_7CONH	$CO_2C_2H_4CH(CH_3)_2$	3.4 ± 1.7
15	2-furyl-CONH	CO_2CH_3	7.0 ± 1.5
16	NH_2	$CO_2(CH_2)_2OH$	60 ± 8

Biological Studies. Metabolism Studies. Metabolism of the lavendamycin analogues by recombinant human NQO1 was examined. Reduction rates by NQO1 were measured using a spectrophotometric assay that employs cytochrome *c* as the terminal electron acceptor[55] and gives initial rates of lavendamycin analogue reduction (Table 5). The initial reduction rates (μmol cytochrome *c* reduced/min/mg NQO1) were calculated from the linear portion (0–30 s) of the reaction graphs.

Compound **12** with the $NHCOCH_3$ and $CONH(CH_2)_3CH_3$ groups at R^1 and R^2 positions, respectively, displayed the highest metabolism rate by NQO1 among the compounds (Table 5). The $NHCOCH_3$ group, a medium size substituent, did not produce steric hindrance with the internal wall of the NQO1 active site, resulting in favorable positioning of **12** for hydride ion reception from FAD and quinone reduction. Our docking studies determined that this group was also capable of hydrogen bonding with FAD and the key residues of the active site. These studies also demonstrated that the $CONH(CH_2)_3CH_3$ group at the R^2 position (pointing toward the outside of the active site) was capable of forming van der Waals interactions with the Phe-232 residue of the NQO1 active site. This could be a contributing factor to the substrate specificity of this compound. Compound **28** with the straight chain *n*-octyl ester substituent at the R^2 position ($CO_2C_8H_{17}$-*n*) was determined to be a good substrate for the enzyme similar to **12**.[8] The docking studies also indicated ligand **12** as a good substrate for NQO1 consistent with the metabolism data.

Although **13** possessed a similar chemical structure to **12** (the best substrate), it was a poor substrate for NQO1 (Table 5) in accordance with the docking data. Compounds **12** and **13** are structural isomers. The $CONH(CH_2)_3CH_3$ group at the R^2 position of **12** is a large, nonbulky, and straight chain aliphatic group, whereas $CONHCH(CH_3)C_2H_5$ at the R^2 position of **13** is a large, bulky, and branched structural isomer of the former. According to our docking studies, the branched configuration at R^2 of **13** was not capable of forming van der Waals interactions with the Phe-232 residue of the NQO1 active site because the *sec*-butyl group is no longer in proximity with the residue due to the inverted orientation of this substrate.

Table 6. Cytotoxicity of Lavendamycin Analogues towards BE (NQO1-Deficient) and BE-NQ (NQO1-Rich) Human Colon Adenocarcinoma Cell Lines

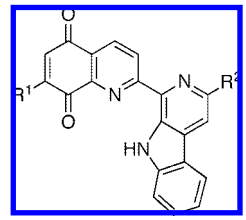

no.	R^1	R^2	cytotoxicity IC_{50} (μM) BE-NQ	cytotoxicity IC_{50} (μM) BE	selectivity ratio [IC_{50} (BE)/IC_{50} (BE-NQ)]
12	CH_3CONH	$CONH(CH_2)_3CH_3$	1.7 ± 0.1	50 ± 2	30
13	CH_3CONH	$CONHCH(CH_3)C_2H_5$	>50	>50	
14	*n*-C_3H_7CONH	$CO_2C_2H_4CH(CH_3)_2$	>50	>50	
15	2-furyl-CONH	CO_2CH_3	47 ± 3	49 ± 7	1
16	NH_2	$CO_2(CH_2)_2OH$	0.5 ± 0.1	3.3 ± 0.2	7

Compound **15** exhibited a low metabolism rate by NQO1 (Table 5) due to the possible failure of the NHCO-2-furyl group at the R^1 position to intercalate between and form van der Waals interactions with the internal wall residues. Docking studies demonstrated that the lack of R^1-substituent intercalation capability led to the unfavorable positioning of **15** and loss of required hydrogen bonding and/or van der Waals interactions with the active site residues. This compound was also ranked as a poor substrate for NQO1 by the docking studies in accordance with the biological data.

Compound **16** with a small NH_2 group at R^1 and $CO_2(CH_2)_2OH$ at R^2 displayed a good reduction rate by the enzyme (Table 5). According to the docking studies, favorable positioning of **16** in the active site was facilitated by lack of steric interactions of the substituents with the residues of the active site and by hydrogen bond formation with FAD and the residues of the NQO1 active site. Our docking studies also indicated high binding affinities for **16**. A previous study determined that good indolequinone substrates for NQO1 including **25** possessed a hydroxymethyl group at the analogous C3 position.[55] Furthermore, compound **24**, which is a good benzoquinone substrate for NQO1, has a CH_2OH group at the C3 position.[2,25] We also determined that compound **29** that possessed an NH_2 group at R^1 and CH_2OH at R^2 was a good substrate for NQO1.[8]

Previously synthesized compound **14** with $NHCOC_3H_7$-*n* and isoamyl ester groups at the R^1 and R^2 positions, respectively, exhibited the lowest metabolism rate by NQO1 and ranked as the poorest substrate (Table 5). The recently studied lavendamycin analogue **30**, 7-*N*-acetyldemethyllavendamycin isoamyl ester,[8] with an acetamide group at the R^1 position and isoamyl ester group at the R^2 position displayed a reduction rate 12-fold higher than **14**. The decreased reduction rate of **14** compared to **30** can be explained by apparent steric hindrance between the quinolinedione moiety of **14** and the NQO1 active site caused by the large $NHCOC_3H_7$-*n* group at R^1 compared to $NHCOCH_3$ in **30**. This steric interaction could result in exclusion of **14** from the active site with subsequent poor hydride ion reception and quinone reduction capability. Compound **14** was also ranked as a poor substrate by our docking studies.

The best substrates were the 2′-$CONH(CH_2)_3CH_3$-7-$NHCOCH_3$ (**12**) and 2′-$CO_2(CH_2)_2OH$-7-NH_2 (**16**) derivatives with reduction rates of 143 ± 11 and 60 ± 8 μmol/min/mg NQO1, respectively (Table 5).

In Vitro Cytotoxicity. Cytotoxicity studies were also performed on the lavendamycin analogues with cell survival being determined by the colorimetric MTT assay. We previously demonstrated an excellent positive linear correlation between the IC_{50} values (the chemosensitivity results) of the clonogenic and MTT assays for lavendamycin analogues.[8] We utilized the BE human colon adenocarcinoma cells stably transfected with human NQO1 cDNA.[25] The BE cells had no measurable NQO1 activity, whereas activity in the transfected cells (BE-NQ) was 337 nmol/min/mg total cell protein using dichlorophenolindophenol as the standard electron acceptor. In this study, the cytotoxicity of the lavendamycin analogues (Table 6) has been compared in these cell lines.

Designed analogues **12** and **16** that were the best substrates for NQO1 (Table 5) were also more toxic to the NQO1-rich BE-NQ cell line than the NQO1-deficient BE cell line (Table 6). Compounds **12** and **16** had the greatest differential toxicity with a selectivity ratio [IC_{50} (BE)/IC_{50} (BE-NQ)] of 30 and 7, respectively (Table 6). Our previous study also determined that good lavendamycin substrates for NQO1 were selectively toxic toward BE-NQ versus BE cells.[8] Compounds **28**, **29**, **31**,[35] and **2**[52] exhibited high selective toxicity toward BE-NQ cells (selectivity ratios = 10, 11, 9, and 9, respectively).[8] Compound **31** was also reported to highly reduce the colony outgrowth of A549 human lung carcinoma cells,[54] and it displayed promising cytotoxic and antitumor activities in the National Cancer Institute's 60-cell line panel and in vivo hollow fiber tumorigenesis assay.[54]

Lavendamycin analogues, **13**, **14**, and **15**, that were poor substrates for NQO1 (Table 5), demonstrated no selective toxicity toward BE-NQ cells or had no measurable cytotoxicity (IC_{50} > 50 μm) (Table 6). Overall, our results suggested that the best lavendamycin substrates for NQO1 were also the most selectively toxic to the high NQO1 BE-NQ cell line compared to NQO1-deficient BE cells, consistent with our previous study.[8] It is important to note, however, that factors other than reduction by NQO1 are most likely involved in the toxicity of the lavendamycins. We are currently studying the cellular effects of the lavendamycin analogues in NQO1-rich and NQO1-deficient cancer cells in an effort to elucidate mechanisms of toxicity.

Conclusions

Specific lavendamycin analogues of novel design were synthesized and biologically evaluated in order to further assess NQO1 SAR substrate qualities. The novel ligands were evaluated a priori with docking studies employing an X-ray derived NQO1 active site computational model to discern explicit

analogue-active site interactions that are critical for ligand substrate qualities. Taken together, the investigation has served to validate the predictive qualities of the NQO1 computational model. The study determined that our structure-based analogue design criteria were valid, resulting in the design of two analogues with high substrate specificity and selective toxicity toward NQO1-rich cells. It also demonstrated that the in silico model of the NQO1 active site correctly distinguished good and poor NQO1 substrates, confirming that the model possessed practical predictive power. Specifically, the addition of NH_2 or $NHCOCH_3$ groups at R^1 and $CO_2(CH_2)_2OH$ or $CONH(CH_2)_3CH_3$ at R^2 had the greatest positive impact on substrate specificity compared to other substituents at these positions. The best substrates were the 2′-$CONH(CH_2)_3CH_3$-7-$NHCOCH_3$ (**12**) and 2′-$CO_2(CH_2)_2OH$-7-NH_2 (**16**) derivatives, which were also the most selectively toxic to the NQO1-rich BE-NQ cell line compared to the NQO1-deficient BE cell line. The docking data were in agreement with the biological results, and therefore the in silico model of the NQO1 active site can be considered predictive and potentially of great value for the discovery and development of new NQO1-directed lavendamycin antitumor agents. Current efforts in our laboratories are utilizing the robust, predictive NQO1 substrate model to iteratively design a third generation of novel analogues with enhanced, selective, and potent antitumor activity.

Experimental Section

Chemistry. General Methods. Chemical reagents and solvents were purchased from Aldrich, Sigma, and Fisher Chemical companies and used as received unless otherwise noted. 1,4-Dioxane, xylene, and anisole were dried and distilled over sodium/benzophenone. Ethanol and chloroform were dried and distilled over CaH_2. DMF was dried over molecular sieves. Ammonium formate was dried in a vacuum desiccator ($CaCl_2$). Melting ranges were recorded with a Thomas-Hoover capillary melting point apparatus. They are in Celsius and are uncorrected. NMR spectra were recorded on a JEOL Eclipse 400 or Varian Gemini 200 spectrophotometer using $CDCl_3$ or DMSO-d_6 with TMS as internal standard. Chemical shifts (δ) are in ppm and coupling constants (J) are in Hz. Low and high resolution mass spectra were obtained at Indiana University Mass Spectrometry Laboratory, Bloomington, IN. Analytical TLC was performed on Baker silica gel and alumina strip with fluorescent indicator. HPLC tracings were obtained with an Alltech Alltima C18 (3 μm, 33 mm × 7 mm) column and Waters HPLC system (2487 Dual λ Absorbance detector, two 515 HPLC pumps, Empower2 software). The solvent program was isocratic acetonitrile:H_2O (80:20 or 70:30) at 1 mL/min. Elemental analyses were performed by Midwest Microlabs, Ltd.

5,7-Diamino-8-hydroxy-2-methylquinolie Dihydrochloride (18). In a 500 mL heavy-walled hydrogenation bottle, finely powdered 8-hydroxy-2-methyl-5,7-dinitroquinoline[52] (**17**, 8.99 g, 3.6 mmol), and 5% Pd/C (2.0 g) were suspended in 135 mL of water, and 15 mL of concentrated hydrochloric acid. In a Parr hydrogenator, this mixture was shaken under 41 psi of hydrogen for 24 h. The reaction mixture was filtered, and the filtrate was evaporated in vacuo to give a bright-orange solid. After drying under vacuum, the pure solid product weighed 7.78 g, (82%): ^{1}H NMR (DMSO-d_6) δ: 2.75 (s, 3H), 3.98–6.10 (br s, 7H), 6.54 (s, 1H), 7.10 (d, 1H, J = 8.06), 8.67 (d, 1H, J = 8.06).

5,7-Difuroylamino-8-hydroxy-2-methylquinoline (19). In a 250 mL two-necked round-bottomed flask equipped with a magnetic stirring bar and an argon balloon, 8-hydroxy-2-methylquinoline-5,7-diammonium dichloride (**18**, 8.00 g, 0.030 mmol), sodium acetate (16 g, 0.20 mol), and sodium sulfite (16.00 g, 0.12 mol) were placed in 60 mL of dry DMF. The solution was stirred and cooled in an ice bath. To this solution, 2-furoyl chloride (6.0 mL, 0.06 mol) was added and stirred in the ice bath for 2 h. The mixture was filtered, and the filtrate was placed in a 2 L beaker containing 850 mL of ice–water (1/2, ice/water). The mixture was allowed to stand at room temperature for 36 h, and the solid was filtered off. Recrystallization of the crude mixture from hot MeOH-H_2O (V/V 20/80), gave pure crystals of **19**, which were dried under vacuum (9.04 g, 75%): mp 246.5–247 °C; R_f = 0.66 (1/20, MeOH/CH_2Cl_2). ^{1}H NMR (DMSO-d_6) δ: 2.74 (s, 3H), 6.75 (dd, 2H, J = 3.4, 1.6), 7.33–7.49 (m, 3H), 7.92–8.16 (m, 4H), 9.52 (s, 1H), 10.34 (s, 1H). HRMS *m/e* calcd for $C_{20}H_{15}N_3O_5$, 377.1012; found, 377.1013.

7-*N*-Furoylamino-2-methylquinoline-5,8-dione (20). In a 500 mL round-bottomed flask equipped with a magnetic stirring bar, 5,7-difuroyl-amino-8-hydroxy-2-methylquinoline (**19**, 2.00 g, 0.005 mol) was suspended in 110 mL of glacial acetic acid and 10 mL of THF. A solution of potassium dichromate (3.10 g, 0.01 mol) in 55 mL of water was added, and the resulting dark solution was stirred at room temperature for 20 h. To the reaction mixture, 100 mL of water was added then was extracted with dichloromethane (12 × 50 mL). The organic extracts were combined and washed with 5% sodium bicarbonate (200 mL) then washed with saturated sodium chloride solution (3 × 100 mL), dried with magnesium sulfate, and evaporated in vacuo to give an orange-yellow product. The solid was washed with 3 mL of acetone to give a light-yellow solid. After drying, the pure product weighed 1.29 g (64.5%): mp 249–250 °C; R_f = 0.75 (1/1 EtOAc/CH_2Cl_2). ^{1}H NMR ($CDCl_3$) δ: 2.79 (s, 3H), 6.63 (dd, 1H, J = 3.5, 1.6), 7.35 (d, 1H, J = 3.3), 7.58 (d, 1H, J = 8.0), 7.65 (d, 1H, J = 2.1), 8.02 (s, 1H), 8.34 (d, 1H, J = 8.0), 9.35 (s, 1H). HRMS *m/e* calcd for $C_{15}H_{10}N_2O_4$, 282.0641; found, 282.0641.

7-Furoylamino-2-formylquinoline-5,8-dione (5). In a 50 mL round-bottomed flask equipped with a magnetic stirring bar, water cooled reflux condenser, and an argon filled balloon was placed 7-furoylamino-2-methylquinoline-5,8-dione (**20**, 1.25 g, 4.42 mmol), selenium dioxide (0.62 g, 5.54 mmol), 19 mL of dry distilled 1,4-dioxane, and 0.55 mL of water. This mixture was stirred and slowly heated to reflux over a 2 h period. The reaction was monitored by TLC and allowed to stir for an addition 26 h until completion. Then 20 mL of 1,4-dioxane was added to the reaction mixture, and this was stirred and refluxed for 15 min. The entire mixture was filtered and the selenium metal was washed with 10 mL of CH_2Cl_2. To the filtrate was added 100 mL of water, and then the aqueous layer was extracted with CH_2Cl_2 (5 × 100 mL). The organic extracts were combined and washed with 100 mL of 5% sodium bicarbonate solution, dried with magnesium sulfate, and then evaporated in vacuo. The product was dried under vacuum overnight and gave a yellow solid weighing 1.23 g (93%): mp 234.5–235 °C; R_f = 0.2 (1/1 EtOAc/CH_2Cl_2). ^{1}H NMR ($CDCl_3$) δ: 6.65 (dd, 1H, J = 3.5, 1.6), 7.39 (d, 1H, J = 8.0), 7.67 (d, 1H, J = 2.1), 8.17 (s, 1H), 8.35 (d, 1H, J = 8.0), 8.66 (d, 1H, J = 8.0), 9.35 (s, 1H), 10.32 (s, 1H). HRMS *m/e* calcd for $C_{15}H_8N_2O_5$, 296.0433; found, 296.0436.

Benzyloxycarbonyltryptophan *n*-Butyl Amide (22). In a 100 mL round-bottomed flask equipped with an argon flow and magnetic stirring bar, benzyloxycarbonyltryptophan succinimide ester[35] (**21**, 435 mg, 1 mmol), *n*-butylamine (0.11 mL, 1 mmol), 0.14 mL of purified triethylamine, 13 mL of absolute ethanol, and 12 mL of chloroform were combined. The reaction mixture was stirred for 1 h at room temperature while monitoring its progress with TLC. Upon completion, the mixture was evaporated in vacuo to give a solid. The solid was dissolved in 90 mL of EtOAc and washed with 30 mL of water, 10% citric acid (2 × 30 mL), and then neutralized with 15 mL of 1N $NaHCO_3$. The organic layer was then washed with 5 mL of water, dried over sodium sulfate, and evaporated under vacuo until a colorless solid was obtained. The product was dried under vacuum at 65 °C for 2 days to give 0.27 g (68%) of **22**: mp 142–143 °C; R_f = 0.80 (1/5 EtOH/EtOAc). ^{1}H NMR ($CDCl_3$) δ: 0.80 (t, 3H, J = 7.0), 1.04–1.26 (m, 4H), 3.04–3.19 (m, 2H), 3.31–3.40 (m, 2H), 4.44–4.47 (m, 1H), 5.12 (s, 2H), 5.5 (br s, 2H), 7.03 (s, 1H), 7.10–7.35 (m, 3H), 7.35 (s, 5H), 8.08 (br s, 1H). HRMS (EI) calcd for $C_{23}H_{27}N_3O_3$, 393.2047; found, 393.2040.

Tryptophan *n*-Butyl Amide (7). In a 50 mL round-bottomed flask equipped with a magnetic stirring bar and argon flow, benzyloxycarbonyltryptophan butyl amide (**22**, 0.5 g, 1.3 mmol)

was suspended in 30 mL of dry methanol. To this mixture, dry ammonium formate (0.26 g, 4.09 mmol) and 10% Pd/C (0.26 g) were added. The mixture was allowed to stir for 30 min. TLC was used to monitor the progress of the reaction. Upon completion, the reaction mixture was filtered and the filter cake was washed with 10 mL of methanol. The filtrate was evaporated in vacuo to nearly dry, and the water bath temperature was then raised to 100 °C to obtain a honey-brown colored gel. The gel was dried under vacuum in a 50−60 °C oil bath for 2 days to give the final product (0.25 g, 77%): mp 74.5–75.0 °C; R_f = 0.37 (1/5 EtOH/EtOAc). ^{1}H NMR ($CDCl_3$) δ: 0.90 (t, 3H, J = 7.2), 1.21−1.49 (m, 4H), 2.85–3.00 (m, 1H), 3.15–3.30 (m, 2H), 3.30−3.50 (m, 1H), 3.67–3.73 (m, 1H), 7.04 (s, 1H), 7.10–7.29 (m, 2H), 7.29–7.36 (m, 1H), 7.38 (d, 1H, J = 7.7), 7.66 (d, 1H, J = 7.7), 8.70 (br s, 1H). HRMS calcd for $C_{15}H_{21}N_3O$, 260.1763; found, 260.1764.

Benzyloxycarbonyltryptophan *sec*-Butyl Amide (23). In a 100 mL round-bottomed flask equipped with an argon flow and magnetic stirring bar was placed benzyloxycarbonyltryptophan succinimide ester[35] (**21**, 0.870 g, 2 mmol), *sec*-butyl amine (0.22 mL, 2 mmol), 0.28 mL of purified triethylamine, 26 mL of absolute ethanol, and 24 mL of chloroform. The reaction mixture was stirred at room temperature for 2 h while monitoring the reaction progress with TLC. Once completed, the mixture was evaporated in vacuo to a dry gel. The product was dissolved in 60 mL of EtOAc and washed with 30 mL of water, 10% citric acid (8 mL), 10 mL of 5% $NaHCO_3$ solution, and then with 8 mL of brine. The organic solution was dried over sodium sulfate overnight and then evaporated under vacuum to dryness. The resulting material was placed under vacuum for 2 days to give a clear-brown gel (0.71 g, 90%); R_f = 0.46 (1/3 EtOAc/$CHCl_3$). ^{1}H NMR ($CDCl_3$) δ: 0.79 (t, 3H, J = 6.6), 0.90 (d, 3H, J = 6.42), 1.24 (t, 2H, J = 8.0), 3.13–3.40 (m, 2H), 3.76 (m, 1H), 4.43 (t, 1H, J = 5.5), 5.12 (s, 2H), 5.20–5.40 (m, 1H) 5.5 (br s, 1H), 7.03 (s, 1H), 7.20–7.28 (m, 2H), 7.30 (d, 1H, J = 6.6), 7.32–7.40 (m, 5H), 7.71 (d, 1H, J = 5.9), 8.10 (br s, 1H). HRMS(EI) calcd for $C_{23}H_{27}N_3O_3$, 393.2047; found, 393.2049.

Tryptophan *sec*-Butyl Amide (8). In a 100 mL round-bottomed flask equipped with a magnetic stirring bar and argon flow was placed benzyloxycarbonyltryptophan *sec*-butyl amide (**23**, 0.5 g, 1.3 mmol) and 30 mL of dry methanol. To this was added dry ammonium formate (0.26 g, 5.5 mmol) and 10% Pd/C (0.26 g). The mixture was allowed to stir for 30 min. TLC was used to observe the completion of the reaction (15 min). The brownish precipitate was filtered, the filter cake was washed with 10 mL of methanol, and the filtrate was evaporated in vacuo to near dryness. The water bath temperature raised to 100 °C to further dry the product and then finally heated under vacuum in a 60 °C oil bath for two days. The product was a white solid and weighed 0.26 g (75%): mp 72–73 °C; R_f = 0.11 (0.2/3/2 MeOH/EtOAc/CH_2Cl_2). ^{1}H NMR ($CDCl_3$) δ: 0.90 (t, 3H, J = 6.8), 1.09 (d, 3H, J = 6.5), 1.39 (m, 2H), 2.90–3.45 (m, 2H), 3.68–3.72 (m, 1H), 3.90 (t, 1H, J = 6.5), 7.01 (s, 1H), 7.12 (d, 1H, J = 8.4), 7.05–7.25 (m, 2H), 7.38 (d, 1H, J = 8.0), 7.71 (d, 1H, J = 8.0), 8.3 (br s, 1H). HRMS (EI) calcd for $C_{15}H_{21}N_3O$, 258.1601; found, 258.1610.

7-*N*-Acetyldemethyllavendamycin *n*-Butyl Amide (12). In a 100 mL three-necked, round-bottomed flask, equipped with a reflux condenser, argon flow, and a magnetic stirring bar, 7-acetamido-2-formylquinoline-5,8-dione (**3**, 36.6 mg, 0.15 mmol), tryptophan *n*-butyl amide (**7**, 38.8 mg, 0.15 mmol), and 60 mL of dry anisole were slowly heated to 165 °C over a 3 h period. The temperature was maintained for an additional 20 h and then the mixture was allowed to cool down to room temperature. The resulting dark-brown precipitate was filtered and washed with a minimal amount of chloroform to give 38 mg (53%) of **12**. Flash chromatography of the crude product ($CHCl_3$) gave an orange solid (31 mg, 43%): mp 243–244 °C; R_f = 0.76 (0.1/5, MeOH/CH_2Cl_2). ^{1}H NMR ($CDCl_3$) δ: 1.03 (t, 3H, J = 7.1), 1.51–1.79 (m, 4H), 2.39 (s, 3H), 3.60–3.63 (m, 2H), 7.39 (dd, 1H, J = 7.4, 7.6), 7.64 (d, 1H, J = 7.7), 7.64 (dd, 1H, J = 7.4, 7.7), 8.00 (s, 1H), 8.00–8.17 (m, 1H), 8.19 (d, 1H, J = 7.3), 8.47 (s, 1H), 8.50 (d, 1H, J = 8.4), 8.89 (d, 1H, J = 8.4), 9.00 (s, 1H), 11.63 (br s, 1H). HRMS *m/e* calcd for $C_{27}H_{23}N_5O_4$, 481.1745; found, 481.1744.

7-*N*-Acetyldemethyllavendamycin *sec*-Butyl Amide (13). In a 250 mL round-bottomed flask equipped with a magnetic stirring bar and Dean–Stark trap were placed 7-acetamido-2-formylquinoline-5,8-dione (109 mg, 0.45 mmol) and tryptophan *sec*-butyl amide (116.4 mg, 0.45 mmol) along with 180 mL of dry anisole. This mixture was stirred and heated, using an oil bath, to 167 °C over a period of 2 h. The solution was refluxed for a total of 15 h, and the completion of the reaction was verified by TLC. The mixture was filtered while hot to remove the brown solid impurity. The filtrate was rotary evaporated to dryness, and the resulting solid was dissolved in a minimal amount of $CHCl_3$ and acetone. This solution was kept at room temperature overnight and then filtered to yield an orange solid (73 mg 35%): mp 306–308 °C; R_f = 0.73 (0.25/5 acetone/$CHCl_3$). ^{1}H NMR ($CDCl_3$) δ: 1.07 (t, 3H, J = 7.44), 1.39 (d, 3H, J = 6.6), 1.60–1.80 (m, 2H), 2.39 (s, 3H), 4.18–4.25 (m, 1H), 7.38–7.48 (m, 1H), 7.63−7.76 (m, 2H), 7.89–7.95 (m, 1H), 8.04 (s, 1H), 8.28 (d, 1H, J = 7.7), 8.49 (br s, 1H), 8.63 (d, 1H, J = 8.4), 9.00 (d, 1H, J = 8.4), 9.10 (s, 1H), 11.80 (br s, 1H). HRMS (EI) calcd for $C_{27}H_{23}N_5O_4$, 481.1745; found, 481.1744.

7-*N*-(2-Furoyl)demethyllavendamycin Methyl Ester (15). In a 50 mL three-necked round-bottomed flask, equipped with a reflux condenser, argon flow, and a magnetic stirring bar was added 7-furoylamino-2-formylquinoline-5,8-dione (**5**, 29.7 mg, 0.1 mmol), L-tryptophan methyl ester (21.8 mg, 0.1 mmol), and 100 mL of dried, distilled xylene. This mixture was slowly heated to 145 °C over a 3 h period and then was maintained at this temperature for an additional 17 h. The reaction mixture was then evaporated in vacuo to give a brownish-orange solid weighing 37.83 mg (77%). This solid was purified by flash chromatography (1/1 $CHCl_3$/THF). The final product was an orange solid weighing 26.32 mg (53.5%): mp 301.5–302.5 °C; R_f = 0.65 (0.1/5 MeOH/CH_2Cl_2). ^{1}H NMR ($CDCl_3$) δ: 3.20 (s, 3H), 4.12 (s, 3H), 6.67(dd, 1H, J = 3.2, 1.4), 7.40–7.45 (dd, 1H, J = 11.6, 8.0), 7.60–7.75 (m, 2H), 7.81 (d, 1H, J = 8.3), 8.13 (s, 1H), 8.27 (d, 1H, J = 8.0), 8.63 (d, 1H, J = 8.4), 9.26 (d, 1H, J = 8.2), 9.44 (s, 1H), 11.92 (br s, 1H). HRMS *m/e* calcd for $C_{27}H_{16}N_4O_6$, 492.1069; found, 492.1063.

Lavendamycin β-Hydroxyethyl Ester (16). In a 25 mL two-necked round-bottomed flask, 7-*N*-acetyldemethyllavendamycin β-hydroxyethyl ester[35] (70.5 mg, 0.15 mmol) was added to 7.2 mL of a 70% solution of sulfuric acid and under an argon atmosphere was stirred and heated to 60 °C for 3.5 h. The reaction mixture was carefully basified with a saturated solution of sodium carbonate to pH = 8 and then evaporated in vacuo to dryness. The residue was extracted with MeOH−CH_2Cl_2 (10 mL/60 mL) and then (5 mL/30 mL). The organic extracts were evaporated in vacuo to a small volume. Vacuum filtration of the resulting precipitate gave the final product as a dark-red solid (18.9 mg (29.5%): mp > 280 °C; R_f = 0.31 (0.3/5 MeOH/CH_2Cl_2). ^{1}H NMR (DMSO-d_6) δ: 3.83 (m, 2H), 4.44 (m, 2H), 5.02 (br s, 2H), 5.96 (s, 1H), 7.36–7.45 (m, 1H), 7.68–7.75 (m, 1H), 7.78 (d, 1H, J = 8.0), 8.51 (d, 1H, J = 8.0), 8.55 (d, 1H, J = 8.1), 8.92 (d, 1H, J = 8.1), 9.12 (s, 1H), 12.01 (br s, 1H). HRMS *m/e* calcd for $C_{23}H_{16}N_4O_5$, 428.1121; found, 428.1136.

Molecular Modeling. In Silico Model of the NQO1 Active Site. The coordinates of the crystal structure of human NQO1 complex with bound FAD and indolequinone **27**, obtained from the Protein Data Bank (PDB ID code: 1H69[45]), were previously utilized as a reference structure to develop the in silico model of the NQO1 active site.[8] Briefly, the physiological dimer in the crystal unit was used for docking purposes. To develop the model, we previously superposed the energy-minimized lavendamycin analogue **29** to the coordinates of the original reference ligand **27** such that the 3D overlap was optimal. Ligand **29** was energy minimized in the context of the active site and therefore the position of the ligand within the pocket was considered optimized for the purpose of this study. The active site was then defined as all the amino acid residues confined within a 6.5 Å radius sphere centered about the superposed ligand **29**. The active site coordinates were locally minimized with attenuated iterations (100) by the Powell standard method, using the Minimize Subset option within SYBYL. This option automatically selected 24 seed amino acid residues sur-

rounding the superposed ligand **29** to perform the local minimization. Default parameters and values within the minimization dialogue were used except where otherwise mentioned. The active site minimization procedure yielded a weighted root-mean-square distance of 0.26 Å between the 24 corresponding residues of interest in the structures. The composite file containing ligand **29** and FAD was saved. The composite structure without ligand **29** was utilized as the in silico model of the NQO1 active site for docking studies. Ligand **29** served as the reference ligand for the docking studies. Docking calculations were performed using one of the two identical active sites.

Ligand Preparation. The structures of ligands were built as MOL2 files employing the Sketch Molecule module of the SYBYL 7.0 software suite[60] (Tripos, Inc., St. Louis, MO). Initially sketched ligands were subjected to energy minimization (10000 iterations) by the Powell minimization standard method. Initial optimization and termination parameters were set to None and Energy Change options, respectively. Default parameters and values within the minimization dialogue (Minimize Details) were used except where otherwise noted. The final ligand conformational coordinates were stored as MOL2 files within the database.

Docking. Flexible docking was performed using the FlexX software module[61,62] within the SYBYL 7.0 environment.[60] The automatic FlexX docking program assessed the conformationally flexible ligands by employing the 3D structure of the target protein in PDB format and was capable of determining 30 possible conformations for each of the docked ligands. The final rank order of conformations was based on the free binding energy. The program automatically selected the base fragment of a ligand (the ligand core). The base fragment was then automatically placed into the active site of the target protein using the FlexX algorithmic pose clustering approach that is based upon a pattern recognition paradigm. Subsequent incremental reconstruction of the complete ligand molecule was then performed by linking the remaining components.[61,62] For the in silico model, the active site was defined as all the amino acid residues confined within a 6.5 Å radius sphere centered on the superposed ligand **29**. FAD was introduced to the active site as a heteroatom file in MOL2 format.

Scoring Functions. The docked conformations of ligands were evaluated and ranked using FlexX and four scoring functions implemented in the CSCORE software module within the SYBYL environment. The CSCORE module allowed consensus scoring that integrated multiple well-known scoring functions such as FlexX, ChemScore,[64] D-Score,[65] G-Score[66] and PMF-Score[67] to evaluate docked ligand conformations. With CSCORE, columns were created in a molecular spreadsheet that contain raw scores for each individual scoring function. The consensus column contained integers that ranged from 0 to 5, where 5 was the best fit to the defined NQO1 model. A CSCORE threshold of ≥ 4 was used to define those poses worthy of post-docking distance and residue contact analyses discussed in the Results Section.

Molecular Graphics. The molecular graphics images were prepared with PyMOL software, version PyMOLX11Hybrid 0.97[68] (Delano Scientific, San Carlos, CA). The data for the coordinates of the NQO1 complex with bound FAD and docked conformations of ligands were prepared in PDB format as PyMOL input files. PyMOL session files of the NQO1 active site with docked conformations of ligands, and the superpositioning of the clustered conformations were created and afforded the images herein and within the Supporting Information.

Biological Studies. Cell Culture. BE human colon adenocarcinoma cells and stably NQO1-transfected BE-NQ cells[69] were a gift from Dr. David Ross (University of Colorado Health Sciences Center, Denver, CO). Cells were grown in minimum essential medium with Earle's salts, nonessential amino acids, L-glutamine, and penicillin/streptomycin and supplemented with 10% fetal bovine serum, sodium bicarbonate, and HEPES. Cell culture medium and supplements were obtained from Gibco, Invitrogen Co. (Grand Island, NY). The cells were incubated at 37 °C under a humidified atmosphere containing 5% CO_2.

Cytochrome *c* Assay. Lavendamycin analogue reduction was monitored using a spectrophotometric assay in which the rate of reduction of cytochrome *c* was quantified at 550 nm. Briefly, the assay mixture contained cytochrome *c* (70 μm), NADH (1 mM), recombinant human NQO1 (0.1–3 μg) (gift from Dr. David Ross, University of Colorado Health Sciences Center, Denver, CO), and lavendamycins (25 μm) in a final volume of 1 mL of Tris-HCl (25 mM, pH 7.4) containing 0.7 mg/mL BSA and 0.1% Tween-20. Reactions were carried out at room temperature and started by the addition of NADH. Rates of reduction were calculated from the initial linear part of the reaction curve (0–30 s), and results were expressed in terms of μmol of cytochrome *c* reduced/min/mg of NQO1 using a molar extinction coefficient of 21.1 mM^{-1} cm^{-1} for cytochrome *c*. All reactions were carried out at least in triplicate.

MTT Assay. Growth inhibition was determined using the MTT colorimetric assay. Cells were plated in 96-well plates at a density of 10000 cells/mL and allowed to attach overnight (16 h). Lavendamycin analogue solutions were applied in medium for 2 h. Lavendamycin analogue solutions were removed and replaced with fresh medium, and the plates were incubated at 37 °C under a humidified atmosphere containing 5% CO_2 for 4–5 days. MTT (50 μg) was added, and the cells were incubated for another 4 h. Medium/MTT solutions were removed carefully by aspiration, the MTT formazan crystals were dissolved in 100 μL of DMSO, and absorbance was determined on a plate reader at 560 nm. IC_{50} values (concentration at which cell survival equals 50% of control) were determined from semilog plots of percent of control vs concentration. Selectivity ratios were defined as the IC_{50} values for the BE cell line divided by the IC_{50} values for the BE-NQ cell line.

Acknowledgment. We acknowledge financial support from the American Cancer Society, the National Institutes of Health (NIH grants: R15 CA78232 and P20 RR017670, H.D.B.; P20 RR15583, J.M.G.; and R15 CA74245, M.B.) and Ball State University. We also would like to acknowledge Colgate-Palmolive/Society of Toxicology for providing us with the graduate student research award in alternative methods (MH). We thank Professor David Williams and the staff at the Mass Spectroscopy Laboratory of Indiana University for their assistance in obtaining mass spectral data. The expert assistance of Rohn Wood of the Molecular Computational Core Facility of The University of Montana is greatly appreciated.

Supporting Information Available: NMR spectra, HPLC tracings, analytical data, geometric postdocking analyses, and molecular models of poses of lavendamycin analogues docked into the NQO1 active site are available free of charge via the Internet at http://pubs.acs.org.

References

(1) Skelly, J. V.; Sanderson, M. R.; Suter, D. A.; Baumann, U.; Read, M. A.; Gregory, D. S.; Bennett, M.; Hobbs, S. M.; Neidle, S. Crystal structure of human DT-diaphorase: A model for interaction with the cytotoxic prodrug 5-(aziridin-1-yl)-2,4-dinitrobenzamide (CB1954). *J. Med. Chem.* **1999**, *42*, 4325–4330.

(2) Danson, S.; Ward, T. H.; Butler, J.; Ranson, M. DT-diaphorase: A target for new anticancer drugs. *Cancer Treat. Rev.* **2004**, *30*, 437–449.

(3) Lind, C.; Cadenas, E.; Hochstein, P.; Ernster, L. DT-diaphorase: Purification, properties, and function. *Methods Enzymol.* **1990**, *186*, 287–301.

(4) Faig, M.; Bianchet, M. A.; Talalay, P.; Chen, S.; Winski, S.; Ross, D.; Amzel, L. M. Structures of recombinant human and mouse NAD(P)H:quinone oxidoreductases: Species comparison and structural changes with substrate binding and release. *Proc. Natl. Acad. Sci. U.S.A.* **2000**, *97*, 3177–3182.

(5) Li, R.; Bianchet, M. A.; Talalay, P.; Amzel, L. M. The three-dimensional structure of NAD(P)H:quinone reductase, a flavoprotein involved in cancer chemoprotection and chemotherapy: Mechanism of the two-electron reduction. *Proc. Natl. Acad. Sci. U.S.A.* **1995**, *92*, 8846–8850.

(6) Ernster, L. DT Diaphorase. *Methods Enzymol.* **1967**, *10*, 309–317.

(7) Ernster, L. DT Diaphorase: A historical review. *Chem. Scripta* **1987**, *27A*, 1–13.
(8) Hassani, M.; Cai, W.; Holley, D. C.; Lineswala, J. P.; Maharjan, B. R.; Ebrahimian, G. R.; Seradj, H.; Stocksdale, M. G.; Mohammadi, F.; Marvin, C. C.; Gerdes, J. M.; Beall, H. D.; Behforouz, M. Novel lavendamycin analogues as antitumor agents: synthesis, in vitro cytotoxicity, structure-metabolism, and computational molecular modeling studies with NAD(P)H:quinone oxidoreductase 1. *J. Med. Chem.* **2005**, *48*, 7733–7749.
(9) Beall, H. D.; Liu, Y.; Siegel, D.; Bolton, E. M.; Gibson, N. W.; Ross, D. Role of NAD(P)H:quinone oxidoreductase (DT-diaphorase) in cytotoxicity and induction of DNA damage by streptonigrin. *Biochem. Pharmacol.* **1996**, *51*, 645–652.
(10) Sun, X.; Ross, D. Quinone-induced apoptosis in human colon adenocarcinoma cells via DT-diaphorase mediated bioactivation. *Chem.−Biol. Interact.* **1996**, *100*, 267–276.
(11) Lewis, A. M.; Ough, M.; Du, J.; Tsao, M. S.; Oberley, L. W.; Cullen, J. J. Targeting NAD(P)H:Quinone oxidoreductase (NQO1) in pancreatic cancer. *Mol. Carcinog.* **2006**, 10.1002/mc.20199 .
(12) Siegel, D.; Gibson, N. W.; Preusch, P. C.; Ross, D. Metabolism of mitomycin C by DT-diaphorase: Role in mitomycin C-induced DNA damage and cytotoxicity in human colon carcinoma cells. *Cancer Res.* **1990**, *50*, 7483–7489.
(13) Siegel, D.; Beall, H. D.; Senekowitsch, C.; Kasai, M.; Arai, H.; Gibson, N. W.; Ross, D. Bioreductive activation of mitomycin C by DT-diaphorase. *Biochemistry* **1992**, *31*, 7879–7885.
(14) Pink, J. J.; Planchon, S. M.; Tagliarino, C.; Varnes, M. E.; Siegel, D.; Boothman, D. A. NAD(P)H:Quinone oxidoreductase activity is the principal determinant of beta-lapachone cytotoxicity. *J. Biol. Chem.* **2000**, *275*, 5416–5424.
(15) Planchon, S. M.; Pink, J. J.; Tagliarino, C.; Bornmann, W. G.; Varnes, M. E.; Boothman, D. A. beta-Lapachone-induced apoptosis in human prostate cancer cells: Involvement of NQO1/xip3. *Exp. Cell Res.* **2001**, *267*, 95–106.
(16) Walton, M. I.; Smith, P. J.; Workman, P. The role of NAD(P)H: quinone reductase (EC 1.6.99.2, DT-diaphorase) in the reductive bioactivation of the novel indoloquinone antitumor agent EO9. *Cancer Commun.* **1991**, *3*, 199–206.
(17) Swann, E.; Barraja, P.; Oberlander, A. M.; Gardipee, W. T.; Hudnott, A. R.; Beall, H. D.; Moody, C. J. Indolequinone antitumor agents: Correlation between quinone structure and rate of metabolism by recombinant human NAD(P)H:quinone oxidoreductase. Part 2. *J. Med. Chem.* **2001**, *44*, 3311–3319.
(18) Beall, H. D.; Winski, S.; Swann, E.; Hudnott, A. R.; Cotterill, A. S.; O'Sullivan, N.; Green, S. J.; Bien, R.; Siegel, D.; Ross, D.; Moody, C. J. Indolequinone antitumor agents: Correlation between quinone structure, rate of metabolism by recombinant human NAD(P)H: quinone oxidoreductase, and in vitro cytotoxicity. *J. Med. Chem.* **1998**, *41*, 4755–4766.
(19) Fisher, G. R.; Gutierrez, P. L. Free radical formation and DNA strand breakage during metabolism of diaziquone by NAD(P)H quinone-acceptor oxidoreductase (DT-diaphorase) and NADPH cytochrome c reductase. *Free Radical Biol. Med.* **1991**, *11*, 597–607.
(20) Ngo, E. O.; Nutter, L. M.; Sura, T.; Gutierrez, P. L. Induction of p53 by the concerted actions of aziridine and quinone moieties of diaziquone. *Chem. Res. Toxicol.* **1998**, *11*, 360–368.
(21) Siegel, D.; Gibson, N. W.; Preusch, P. C.; Ross, D. Metabolism of diaziquone by NAD(P)H:(quinone acceptor) oxidoreductase (DT-diaphorase): Role in diaziquone-induced DNA damage and cytotoxicity in human colon carcinoma cells. *Cancer Res.* **1990**, *50*, 7293–7300.
(22) Nemeikaite-Ceniene, A.; Dringeliene, A.; Sarlauskas, J.; Cenas, N. Role of NAD(P)H:quinone oxidoreductase (NQO1) in apoptosis induction by aziridinylbenzoquinones RH1 and MeDZQ. *Acta Biochim. Pol.* **2005**, *52*, 937–941.
(23) Dehn, D. L.; Inayat-Hussain, S. H.; Ross, D. RH1 induces cellular damage in an NAD(P)H:quinone oxidoreductase 1-dependent manner: Relationship between DNA cross-linking, cell cycle perturbations, and apoptosis. *J. Pharmacol. Exp. Ther.* **2005**, *313*, 771–779.
(24) Dehn, D. L.; Winski, S. L.; Ross, D. Development of a new isogenic cell-xenograft system for evaluation of NAD(P)H:quinone oxidoreductase-directed antitumor quinones: evaluation of the activity of RH1. *Clin. Cancer Res.* **2004**, *10*, 3147–3155.
(25) Winski, S. L.; Hargreaves, R. H.; Butler, J.; Ross, D. A new screening system for NAD(P)H:quinone oxidoreductase (NQO1)-directed antitumor quinones: Identification of a new aziridinylbenzoquinone, RH1, as a NQO1-directed antitumor agent. *Clin. Cancer Res.* **1998**, *4*, 3083–3088.
(26) Cresteil, T.; Jaiswal, A. K. High levels of expression of the NAD(P)H: quinone oxidoreductase (NQO1) gene in tumor cells compared to normal cells of the same origin. *Biochem. Pharmacol.* **1991**, *42*, 1021–1027.
(27) Malkinson, A. M.; Siegel, D.; Forrest, G. L.; Gazdar, A. F.; Oie, H. K.; Chan, D. C.; Bunn, P. A.; Mabry, M.; Dykes, D. J.; Harrison, S. D.; Ross, D. Elevated DT-diaphorase activity and messenger RNA content in human non-small cell lung carcinoma: Relationship to the response of lung tumor xenografts to mitomycin C. *Cancer Res.* **1992**, *52*, 4752–4757.
(28) Mikami, K.; Naito, M.; Ishiguro, T.; Yano, H.; Tomida, A.; Yamada, T.; Tanaka, N.; Shirakusa, T.; Tsuruo, T. Immunological quantitation of DT-diaphorase in carcinoma cell lines and clinical colon cancers: Advanced tumors express greater levels of DT-diaphorase. *Jpn. J. Cancer Res.* **1998**, *89*, 910–915.
(29) Rampling, R.; Cruickshank, G.; Lewis, A. D.; Fitzsimmons, S. A.; Workman, P. Direct measurement of pO2 distribution and bioreductive enzymes in human malignant brain tumors. *Int. J. Radiat. Oncol. Biol. Phys.* **1994**, *29*, 427–431.
(30) Schlager, J. J.; Powis, G. Cytosolic NAD(P)H:(quinone-acceptor) oxidoreductase in human normal and tumor tissue: Effects of cigarette smoking and alcohol. *Int. J. Cancer* **1990**, *45*, 403–409.
(31) Balitz, D. M.; Bush, J. A.; Bradner, W. T.; Doyle, T. W.; O'Herron, F. A.; Nettleton, D. E. Isolation of lavendamycin, a new antibiotic from Streptomyces lavendulae. *J. Antibiot. (Tokyo)* **1982**, *35*, 259–265.
(32) Doyle, T. W.; Balitz, D. M.; Grulich, R. E.; Nettleton, D. E.; Gould, S. J.; Tann, C.; Moews, A. E. Structure determination of lavendamycin, a new antitumor antibiotic from *Streptomyces lavendulae*. *Tetrahedron Lett.* **1981**, *22*, 4595–4598.
(33) Boger, D. L.; Yasuda, M.; Mitscher, L. A.; Drake, S. D.; Kitos, P. A.; Thompson, S. C. Streptonigrin and lavendamycin partial structures. Probes for the minimum, potent pharmacophore of streptonigrin, lavendamycin, and synthetic quinoline-5,8-diones. *J. Med. Chem.* **1987**, *30*, 1918–1928.
(34) Behforouz, M.; Cai, W.; Mohammadi, F.; Stocksdale, M. G.; Gu, Z.; Ahmadian, M.; Baty, D. E.; Etling, M. R.; Al-Anzi, C. H.; Swiftney, T. M.; Tanzer, L. R.; Merriman, R. L.; Behforouz, N. C. Synthesis and evaluation of antitumor activity of novel *N*-acyllavendamycin analogues and quinoline-5,8-diones. *Bioorg. Med. Chem.* **2007**, *15*, 495–510.
(35) Behforouz, M.; Cai, W.; Stocksdale, M. G.; Lucas, J. S.; Jung, J. Y.; Briere, D.; Wang, A.; Katen, K. S.; Behforouz, N. C. Novel lavendamycin analogues as potent HIV-reverse transcriptase inhibitors: Synthesis and evaluation of anti-reverse transcriptase activity of amide and ester analogues of lavendamycin. *J. Med. Chem.* **2003**, *46*, 5773–5780.
(36) Fourie, J.; Oleschuk, C. J.; Guziec, F., Jr.; Guziec, L.; Fiterman, D. J.; Monterrosa, C.; Begleiter, A. The effect of functional groups on reduction and activation of quinone bioreductive agents by DT-diaphorase. *Cancer Chemother. Pharmacol.* **2002**, *49*, 101–110.
(37) Gane, P. J.; Dean, P. M. Recent advances in structure-based rational drug design. *Curr. Opin. Struct. Biol.* **2000**, *10*, 401–404.
(38) Joseph-McCarthy, D. Computational approaches to structure-based ligand design. *Pharmacol. Ther.* **1999**, *84*, 179–191.
(39) Kuntz, I. D. Structure-based strategies for drug design and discovery. *Science* **1992**, *257*, 1078–1082.
(40) Suleman, A.; Skibo, E. B. A comprehensive study of the active site residues of DT-diaphorase: Rational design of benzimidazolediones as DT-diaphorase substrates. *J. Med. Chem.* **2002**, *45*, 1211–1220.
(41) Erickson, J. A.; Jalaie, M.; Robertson, D. H.; Lewis, R. A.; Vieth, M. Lessons in molecular recognition: the effects of ligand and protein flexibility on molecular docking accuracy. *J. Med. Chem.* **2004**, *47*, 45–55.
(42) Lyne, P. D. Structure-based virtual screening: An overview. *Drug Discovery Today.* **2002**, *7*, 1047–1055.
(43) Kontoyianni, M.; McClellan, L. M.; Sokol, G. S. Evaluation of docking performance: Comparative data on docking algorithms. *J. Med. Chem.* **2004**, *47*, 558–565.
(44) Asher, G.; Dym, O.; Tsvetkov, P.; Adler, J.; Shaul, Y. The crystal structure of NAD(P)H quinone oxidoreductase 1 in complex with its potent inhibitor dicoumarol. *Biochemistry* **2006**, *45*, 6372–6378.
(45) Faig, M.; Bianchet, M. A.; Winski, S.; Hargreaves, R.; Moody, C. J.; Hudnott, A. R.; Ross, D.; Amzel, L. M. Structure-based development of anticancer drugs: Complexes of NAD(P)H:quinone oxidoreductase 1 with chemotherapeutic quinones. *Structure* **2001**, *9*, 659–667.
(46) Winski, S. L.; Faig, M.; Bianchet, M. A.; Siegel, D.; Swann, E.; Fung, K.; Duncan, M. W.; Moody, C. J.; Amzel, L. M.; Ross, D. Characterization of a mechanism-based inhibitor of NAD(P)H:quinone oxidoreductase 1 by biochemical, x-ray crystallographic, and mass spectrometric approaches. *Biochemistry* **2001**, *40*, 15135–15142.
(47) Zhou, Z.; Fisher, D.; Spidel, J.; Greenfield, J.; Patson, B.; Fazal, A.; Wigal, C.; Moe, O. A.; Madura, J. D. Kinetic and docking studies of the interaction of quinones with the quinone reductase active site. *Biochemistry* **2003**, *42*, 1985–1994.
(48) Cavelier, G.; Amzel, L. M. Mechanism of NAD(P)H:quinone reductase: Ab initio studies of reduced flavin. *Proteins: Struct., Funct., Genet.* **2001**, *43*, 420–432.

(49) Chen, S.; Wu, K.; Zhang, D.; Sherman, M.; Knox, R.; Yang, C. S. Molecular characterization of binding of substrates and inhibitors to DT-diaphorase: Combined approach involving site-directed mutagenesis, inhibitor-binding analysis, and computer modeling. *Mol. Pharmacol.* **1999**, *56*, 272–278.
(50) Kende, A. S.; Ebetino, F. H. The regiospecific total synthesis of lavendamycin methyl ester. *Tetrahedron Lett.* **1984**, *25*, 923–926.
(51) Boger, D. L.; Duff, S. R.; Panek, J. S.; Yasuda, M. Total synthesis of lavendamycim methyl ester. *J. Org. Chem.* **1985**, *50*, 5790–5795.
(52) Behforouz, M.; Gu, Z.; Cai, W.; Horn, M. A.; Ahmadian, M. A highly concise synthesis of lavendamycin methyl ester. *J. Org. Chem.* **1993**, *58*, 7089–7091.
(53) Behforouz, M.; Haddad, J.; Cai, W.; Arnold, M. B.; Mohammadi, F.; Sousa, A. C.; Horn, M. A. Highly efficient and practical syntheses of lavendamycin methyl ester and related novel quinolindiones. *J. Org. Chem.* **1996**, *61*, 6552–6555.
(54) Fang, Y.; Linardic, C. M.; Richardson, D. A.; Cai, W.; Behforouz, M.; Abraham, R. T. Characterization of the cytotoxic activities of novel analogues of the antitumor agent, lavendamycin. *Mol. Cancer Ther.* **2003**, *2*, 517–526.
(55) Phillips, R. M.; Naylor, M. A.; Jaffar, M.; Doughty, S. W.; Everett, S. A.; Breen, A. G.; Choudry, G. A.; Stratford, I. J. Bioreductive activation of a series of indolequinones by human DT-diaphorase: Structure−activity relationships. *J. Med. Chem.* **1999**, *42*, 4071–4080.
(56) Jaffar, M.; Phillips, R. M.; Williams, K. J.; Mrema, I.; Cole, C.; Wind, N. S.; Ward, T. H.; Stratford, I. J.; Patterson, A. V. 3-Substituted-5-aziridinyl-1-methylindole-4,7-diones as NQO1-directed antitumour agents: Mechanism of activation and cytotoxicity in vitro. *Biochem. Pharmacol.* **2003**, *66*, 1199–1206.
(57) Hendriks, H. R.; Pizao, P. E.; Berger, D. P.; Kooistra, K. L.; Bibby, M. C.; Boven, E.; Dreef-van der Meulen, H. C.; Henrar, R. E. C.; Fiebig, H. H.; Double, J. A.; Hornstra, H. W.; Pinedo, H. M.; Workman, P.; Schwartsmann, G. EO9: A novel bioreductive alkylating indoloquinone with preferential solid tumour activity and lack of bone marrow toxicity in preclinical models. *Eur. J. Cancer* **1993**, *29A*, 897–906.
(58) Phillips, R. M.; Jaffar, M.; Maitland, D. J.; Loadman, P. M.; Shnyder, S. D.; Steans, G.; Cooper, P. A.; Race, A.; Patterson, A. V.; Stratford, I. J. Pharmacological and biological evaluation of a series of substituted 1,4-naphthoquinone bioreductive drugs. *Biochem. Pharmacol.* **2004**, *68*, 2107–2116.
(59) Kremer, W. B.; Laszlo, J. Comparison of biochemical effects of isopropylidine azastreptonigrin (NSC-62709) with streptonigrin (NSC-45383). *Cancer Chemother. Rep.* **1967**, *51*, 19–24.
(60) *SYBYL Molecular Modeling Software*, version SYBYL 7.0; Tripos Inc.: St. Louis, MO, 2004.
(61) Lemmen, C.; Lengauer, T. Time-efficient flexible superposition of medium-sized molecules. *J. Comput.-Aided Mol. Des.* **1997**, *11*, 357–368.
(62) Rarey, M.; Kramer, B.; Lengauer, T.; Klebe, G. A fast flexible docking method using an incremental construction algorithm. *J. Mol. Biol.* **1996**, *261*, 470–489.
(63) Skibo, E. B.; Gordon, S.; Bess, L.; Boruah, R.; Heileman, M. J. Studies of pyrrolo[1,2-alpha]benzimidazolequinone DT-diaphorase substrate activity, topoisomerase II inhibition activity, and DNA reductive alkylation. *J. Med. Chem.* **1997**, *40*, 1327–1339.
(64) Eldridge, M. D.; Murray, C. W.; Auton, T. R.; Paolini, G. V.; Mee, R. P. Empirical scoring functions: I. The development of a fast empirical scoring function to estimate the binding affinity of ligands in receptor complexes. *J. Comput.-Aided Mol. Des.* **1997**, *11*, 425–445.
(65) Kuntz, I. D.; Blaney, J. M.; Oatley, S. J.; Langridge, R.; Ferrin, T. E. A geometric approach to macromolecule-ligand interactions. *J. Mol. Biol.* **1982**, *161*, 269–288.
(66) Jones, G.; Willett, P.; Glen, R. C.; Leach, A. R.; Taylor, R. Development and validation of a genetic algorithm for flexible docking. *J. Mol. Biol.* **1997**, *267*, 727–748.
(67) Muegge, I.; Martin, Y. C. A general and fast scoring function for protein−ligand interactions: A simplified potential approach. *J. Med. Chem.* **1999**, *42*, 791–804.
(68) DeLano, W. L. *The PyMOL Molecular Graphics System*; versionPyMOL X11Hybrid; DeLano Scientific: San Carlos, CA, 2004.
(69) Winski, S. L.; Swann, E.; Hargreaves, R. H.; Dehn, D. L.; Butler, J.; Moody, C. J.; Ross, D. Relationship between NAD(P)H:quinone oxidoreductase 1 (NQO1) levels in a series of stably transfected cell lines and susceptibility to antitumor quinones. *Biochem. Pharmacol.* **2001**, *61*, 1509–1516.

JM701066A